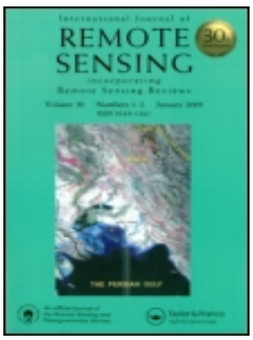

International Journal of Remote Sensing

ISSN: 0143-1161 (Print) 1366-5901 (Online) Journal homepage: http://www.tandfonline.com/loi/tres20

# The application of polynomial analyses to detect global vegetation dynamics during 1982–2012

Yanxu Liu, Yanglin Wang, Yueyue Du, Mingyue Zhao & Jian Peng

**To cite this article:** Yanxu Liu, Yanglin Wang, Yueyue Du, Mingyue Zhao & Jian Peng (2016) The application of polynomial analyses to detect global vegetation dynamics during 1982–2012, International Journal of Remote Sensing, 37:7, 1568-1584, DOI: 10.1080/01431161.2016.1142688

**To link to this article:** http://dx.doi.org/10.1080/01431161.2016.1142688

INTERNATIONAL JOURNAL OF REMOTE SENSING, 2016
VOL. 37, NO. 7, 1568–1584
http://dx.doi.org/10.1080/01431161.2016.1142688

Taylor & Francis
Taylor & Francis Group

# The application of polynomial analyses to detect global vegetation dynamics during 1982–2012

Yanxu Liu, Yanglin Wang, Yueyue Du, Mingyue Zhao and Jian Peng

Laboratory for Earth Surface Processes of the Ministry of Education, College of Urban and Environmental Sciences, Peking University, Beijing, China

**ABSTRACT**

Use of the normalized difference vegetation index (NDVI) to build long-term vegetation trends is one of the most effective techniques for identifying global environmental change. Trend identification can be achieved by ordinary least squares (OLS) analysis or the Theil–Sen (TS) procedure with a Mann–Kendall (MK) significance test, and these linear regression approaches have been widely used. However, vegetation changes are not linear, and thus the response of vegetation to global climate change may follow non-linear trends. In this article, a polynomial trend-fitting method, which uses stepwise regression and expands on previous research, is presented. With an improved fitting ability, this procedure may reveal trends that were concealed by linear fitting methods. Globally, the traditional TS-MK method reveals significant greening trends for 37.27% of vegetated land, and significant browning trends for 7.98%. Using the polynomial analysis, 34.62% of pixels were fitted by high-order trends. The significant greening trends covered up to 30% of cultivated land, thus indicating that cultivated vegetation may be increasing faster than natural vegetation. Significant vegetation browning mostly occurred in sparse vegetation areas, which suggests that vegetation growth may be more sensitive to climate change in arid regions. Our results show that use of polynomial analysis can help further elucidate global NDVI trends.

**ARTICLE HISTORY**
Received 24 May 2015
Accepted 3 January 2016



## 1. Introduction

Vegetation plays a critical role in regulating carbon and maintaining the stability of the climate on a global scale, and the monitoring of vegetation dynamics has been recognized as a key issue in global environmental change research (de Jong et al. 2013; Peng et al. 2012). The most common method used to monitor vegetation on global and regional scales is satellite-based estimations of vegetation indices (Nemani et al. 2003; Running et al. 2004). The normalized difference vegetation index (NDVI) is a satellite-based indicator of vegetation greenness that has been widely applied to describe the spatiotemporal characteristics of green cover (Gao et al. 2012; Hwang et al. 2011; Lanorte et al. 2014; Tucker 1979; Tucker et al. 2001), and determining long-term trends

**CONTACT** Yanglin Wang ylwang@urban.pku.edu.cn Laboratory for Earth Surface Processes of the Ministry of Education, College of Urban and Environmental Sciences, Peking University, Beijing, China

in the NDVI is an effective way of detecting vegetation variability under global environmental change (Jiang et al. 2013; Nie et al. 2012; Stow et al. 2007; Weiss et al. 2004). However, as the results depend largely on the remote sensors and regression algorithms used, the results of global NDVI trend analysis are often controversial (Alcaraz-Segura et al. 2010; Fensholt and Proud 2012; Steven et al. 2003; Wessels, van den Bergh, and Scholes 2012).

A significant issue that should be addressed involves the NDVI trend-fitting method (Verbesselt et al. 2010a, 2010b; Verbesselt, Zeileis, and Herold 2012). ordinary least squares (OLS) regression is a widely used method for determining the relationship between the spatiotemporal characteristics of the NDVI and the driving factors (Bao et al. 2014; Ju et al. 2010; Li et al. 2013; Liu et al. 2014; Mao et al. 2012; Rocchini and Vannini 2010). Meanwhile, the NDVI data adopted from satellite sensors often contain noise, which cannot be eliminated from the non-robust least squares algorithm in OLS. However, several techniques can be used to decompose time series in order to eliminate the noise (Rios et al. 2015). Common methods for processing NDVI data include singular spectrum analysis (Ma et al. 2013; Cañón, Domínguez, and Valdes 2011), Fourier transform (Yan et al. 2015; Kleynhans et al. 2010), wavelets (Mishra, Crews, and Neuenschwander 2012; Martínez and Gilabert 2009), and empirical mode decomposition (Kandasamy et al. 2013; Tucker et al. 2005), and these methods can effectively extract the shape of the non-linearity from the data. Therefore, both non-linearity and noise should be considered during the selection of an appropriate method for processing NDVI time series.

Use of nonparametric regression has been shown to be an effective way to reduce noise (Theil 1950). Recently, a few studies have applied a combination of the Theil–Sen (TS) median slope trend analysis and the Mann–Kendall (MK) monotonic test instead of OLS linear regression (Fensholt et al. 2012; Schucknecht et al. 2013). The TS estimator of a set of two-dimensional points is the median of the slopes determined by all pairs of sample points (Theil 1950). The adoption of the nonparametric TS regression ensures that vegetation trends are robust with respect to outliers and reduces the effects of sensor measurement errors (Fernandes and Leblanc 2005). This procedure can be applied on the raw NDVI series with no need to smooth data (Fuller and Wang 2014). Compared with the computationally intensive smoothing algorithms, significant increases or decreases in the NDVI for each pixel can be detected quickly through the TS–MK combination method (Fensholt et al. 2012; Guay et al. 2014; Neeti and Eastman 2011).

However, it should be noted that the overwhelming majority of NDVI series are non-linear, whereas the TS median slope trend is a robust linear regression procedure. Therefore, some sharp changes over a short period of time may be 'latent' in the relatively low slope of an overall trend. High-order regression involves the application of stepwise selection algorithms that can determine non-linear vegetation trends. Jamali et al. (2014) applied high-order regression models to map the latent trends with polynomials over the Sahel in Africa. Compared with decomposition methods applied to 10 day and monthly data, the high-order regression was shown to be effective for detecting inter-annual changes in non-linear NDVI series.

To further detect the latent change pixels in non-linear shifts, it would be beneficial to test for global latent change pixels with an improved algorithm. This study attempted to

do that, and the data were used to detect the different trend types for typical regions and land-cover types across the globe. The overall aims of this study were to improve the trend classification scheme and to explore new regional disparities in global vegetation dynamics.

## 2. Methods

### 2.1. *Data and processing*

Among the NDVI data sets derived from different satellite sensors, the Global Inventory Modeling and Mapping Studies (GIMMS) NDVI data set, which begins in 1981, is suitable for describing long-term vegetation dynamics (Beck et al. 2011; de Jong et al. 2011; Forkel et al. 2013; Tucker et al. 2005). Its recent successor, GIMMS3g, has been found to be in overall acceptable agreement with Moderate Resolution Imaging Spectroradiometer (MODIS) NDVI data (Fensholt and Proud 2012). Notably, the GIMMS3g data set showed statistically significant ($p$ = 0.05) increases in vegetation productivity over 15% of the high northern latitudes, which is a trend that was not detected in the predecessor GIMMSg data set (Guay et al. 2014). As high spatial resolution is not a strict requirement for global-scale studies, the GIMMS3g data set with a 1/12-degree resolution does provide a good data source for projects involved with the mapping of global vegetation dynamics (Tian et al. 2015).

The GIMMS3g NDVI data were downloaded from Eco Cast for the period from 1982 to 2012 (http://ecocast.arc.nasa.gov/data/pub/gimms/). In this study, the maximum value composite (MVC) method was adopted to generate the annual NDVI for the 31 year study period. This common method is capable of minimizing atmospheric effects, scan angle effects, cloud contamination, and solar zenith angle effects (Holben 1986; Peng et al. 2012). Specifically, the MVC method focuses on the highest biomass month in a year. Here, the maximum NDVI values lower than 0.2 were removed as they represented mostly bare areas.

The global land-cover map GlobCover 2009 was obtained from the European Space Agency (ESA; http://due.esrin.esa.int). This land-cover map includes 22 land-cover types for the year 2009, and data are provided at a spatial resolution of 300 m (Bicheron et al. 2011), which is higher than that of the widely used MODIS V005 Global 500 m Land Cover Type Product MCD12Q1.GlobCover 2009 was used here to analyse trends in various land-cover types.

### 2.2. *Trend estimation*

This study employed an improved approach whereby vegetation variations were divided into cubic, quadratic, linear, and concealed trends with an algorithm during trend estimation. Additionally, insignificant trends were defined as fluctuations. The concealed trends were defined as valid cubic or quadratic trends with statistically insignificant linear slope coefficients, which means that there was no apparent increase or decrease over the whole period, but patterns of change did exist within the annual NDVI series (Jamali et al. 2014). The introduction of cubic and quadratic trends was in response to the observation that a better fit can be achieved for some NDVI series by higher-order

polynomials compared with traditional linear regression procedures. Based on the fitting equation,

$$Y = a_0 + a_1 x + a_2 x^2 + a_3 x^3, \tag{1}$$

where $x$ is the year order, $Y$ is the annual NDVI, and $a_0$, $a_1$, $a_2$, $a_3$ are the coefficients, stepwise regression was introduced in the algorithm and the choice of predictive variables was made by an automatic procedure. Compared with the selection of cubic or quadratic coefficients based on their significance, stepwise regression in this study involved significance tests both for all coefficients used in the model and for the regression model itself. The goal of the stepwise regression was to choose a small subset from the larger set of variables so that the resulting regression model was simple, yet retained a good predictive ability. In other words, the $R^2$ for a cubic regression model could be higher than that for a linear regression model, but if the coefficient was insignificant, the variable may act as an irrelevant regressor. Thus, the objective of the stepwise regression was not to obtain the highest value of $R^2$ but to determine the simplest and best-fit regression.

The variables $x$, $x^2$, and $x^3$ and coefficient selection depended on the $F$-test in this study. In particular, we used a stepwise linear regression model where high-order regressors were considered as variables. Thus, the fitting equation was simplified to $Y = a_0 + a_1x_1 + a_2x_2 + a_3x_3$ ($x_1 = x$, $x_2 = x^2$, $x_3 = x^3$, where $x$ ranged from 1 to 31). Then, a backward selection model was used beginning with all of the candidate variables in the model and we discarded the least significant variable at each step. This process continued until no insignificant ($p \geq 0.05$) variables remained. Moreover, if the high-order coefficients were both insignificant, the fitting equation was simplified to a linear regression, which is a common technique used in vegetation dynamic research.

Specifically, we used the TS procedure with an MK significance test to fit the NDVI change trends and used the results as a cross-reference for comparison with the stepwise regression results. We set the significance level at $p < 0.05$ and realized both TS–MK and stepwise algorithms in MATLAB R2012a (MathWorks). The formulas for the TS–MK procedure are described below.

The TS slope estimator is the median of the slopes calculated between observation values for all pairwise time steps, namely between observations $X_j$ and $X_i$ at pairwise time steps $t_j$ and $t_i$ as follows (Sen 1968; Theil 1950):

$$\text{slope} = \text{Median}\left(\frac{X_j - X_i}{t_j - t_i}\right). \tag{2}$$

For NDVI variations, *slope* > 0 represents revegetation and *slope* < 0 represents vegetation degradation or deterioration.

Similar to the TS procedure, the MK test examines the slopes between all pairwise combinations of samples, where the indicator, Kendall's $S$, is defined as follows (Kendall 1962, 1975; Mann 1945; Neeti and Eastman 2011):

$$S = \sum_{i=1}^{n-1} \sum_{j=i+1}^{n} \text{sign}\left(x_i - x_j\right), \tag{3}$$

$$\operatorname{sign}(x_i - x_j) = \begin{cases} 1 & \text{if} \quad x_i - x_j < 0 \\ 0 & \text{if} \quad x_i - x_j = 0 \\ -1 & \text{if} \quad x_i - x_j > 0 \end{cases}. \tag{4}$$

Here, $n$ is the length of the time series and $x_i$ and $x_j$ are observations at times $i$ and $j$, respectively. When there are independent and identical distributions among data values, the variance is derived as follows:

$$\operatorname{Var}(S) = \frac{n(n-1)(2n+5)}{18} = \sigma^2, \tag{5}$$

where $\sigma$ is the standard deviation and $\operatorname{Var}(S)$ is the covariance of $S$. The equation for MK significance ($Z$) is then computed as follows:

$$Z = \begin{cases} \frac{S-1}{\sqrt{\operatorname{Var}(S)}} & \text{for} \quad S > 0 \\ 0 & \text{for} \quad S = 0 \\ \frac{S+1}{\sqrt{\operatorname{Var}(S)}} & \text{for} \quad S < 0 \end{cases}. \tag{6}$$

In this study, $|Z| > 1.96$ (equivalent to $p < 0.05$) was judged as significant.

### 2.3. *Trend classification scheme*

Based on our polynomial analysis method, the general scheme consisted of a four-phase procedure that distinguished among the following five trend classes: cubic, quadratic, significant linear change, insignificant linear change, and concealed (Figure 1). First, the backward selection stepwise regression and the TS–MK procedure were operated independently, and the TS slope with the $Z$-test for linear regression was also obtained. If both $a_2$ and $a_3$ were 0, the high orders were eliminated and the fitting equation was simplified to a linear regression. Second, the pixels that were neither of a high order nor significant in the MK $Z$-test were classified into the greening or browning classes, the pixels that were not of a high order but were significant in the MK $Z$-test were classified into the significant greening or browning classes, and the pixels that were of a high order but were insignificant in the MK $Z$-test were extracted as the concealed class. Third, the pixels that were both of a high order and significant in the MK $Z$-test were separated into two classes. If $a_3$ was non-zero, the pixels were classified into the cubic class; otherwise, pixels were classified into the quadratic class. Finally, the five trend classes were further divided, whereby the two high-order classes were defined as cubic or quadratic and, depending on the signs of positive or negative attributes of $a_2$ and $a_3$, these trends were further classified as quadratic down-up, quadratic up-down, cubic up-down-up, or cubic down-up-down trends.

### 2.4. *Distinguishing trend types across regions and land-cover types*

The three defined statistical levels included the global level, the national and regional level, and the land-cover level. On the global level, the new results were mapped and compared with calculations from the traditional TS–MK procedure. The regional level encompassed several bordered countries, while the national level only described nations with large areas. The eight nations selected for analysis included Russia, Canada, China,

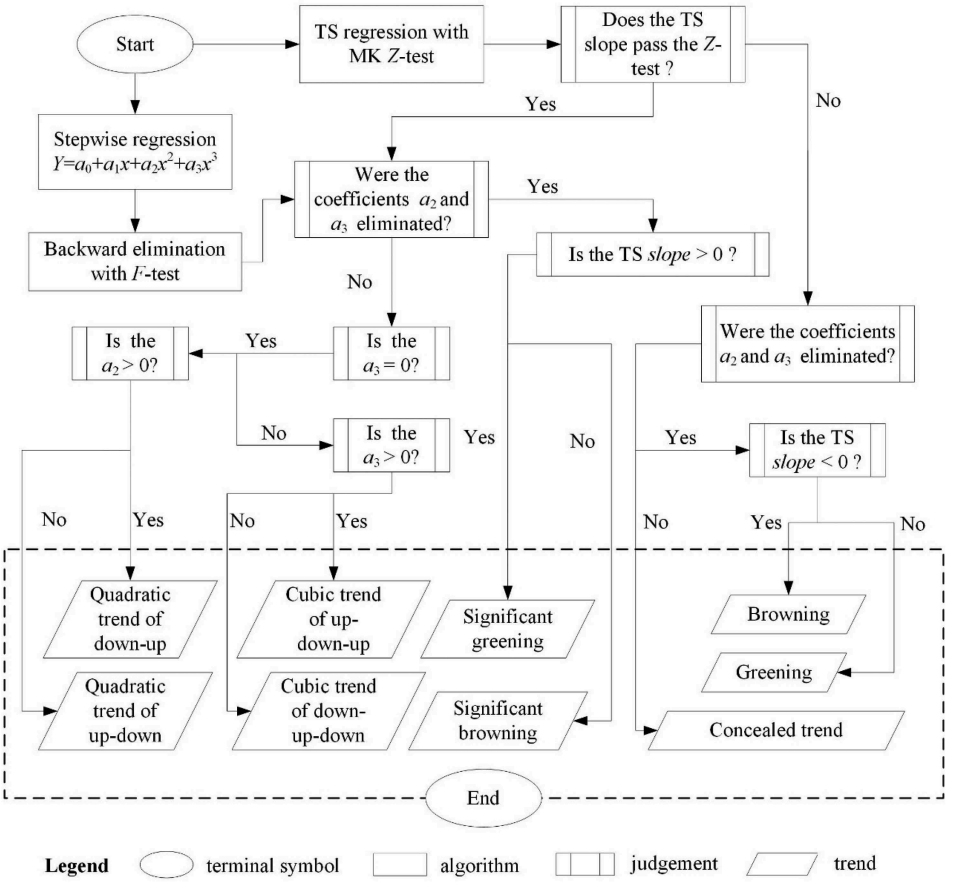


**Figure 1.** Flow chart of the trend classification scheme (TS, Theil–Sen; MK, Mann–Kendall).

USA, Brazil, Australia, India, and Argentina. The supplementary regions that do not include large-area countries were Europe, southeastern Asia, central Asia, western Asia, northern Africa, eastern Africa, western Africa, central Africa, and southern Africa.

On the land-cover level, the land-cover types that showed a scattered distribution or were present in relatively small quantities were merged, thus simplifying the 22 land-cover types of the GlobCover 2009 map to 11 typical types (Table 1). The typical cover types included several major global vegetation types such as broad-leaved forest, needle-leaved forest, shrublands, grasslands, crops, and bare areas (Figure 2). This combination allowed woody, herbaceous, and cultivated vegetation to be distinguished, which may be associated with different change trends.

## 3. Results

### 3.1. *Trends on a global scale*

For the traditional TS–MK method, the ratio between pixels showing significant greening and those showing significant browning was approximately 4.5:1, and

**Table 1.** Typical land-cover types merged from the land-cover types in the GlobCover 2009 map (Bicheron et al. 2011).

| Typical cover type (abbreviated) | Original land-cover types in the GlobCover 2009 map |
|---|---|
| Crop | Irrigated croplands and rain-fed croplands |
| Crop veg | Mosaic croplands/vegetation and mosaic vegetation/croplands |
| Broad evergreen | Closed to open broad-leaved evergreen or semi-deciduous forest |
| Closed broad | Closed broad-leaved deciduous forest |
| Open broad | Open broad-leaved deciduous forest |
| Closed needle | Closed needle-leaved evergreen forest |
| Open needle | Open needle-leaved deciduous or evergreen forest |
| Shrub | Closed to open shrubland |
| Grass | Closed to open grassland |
| Sparse veg | Sparse vegetation |
| Bare areas | Bare areas |

Closed (>40%), open (15–40%), closed to open (>15%).

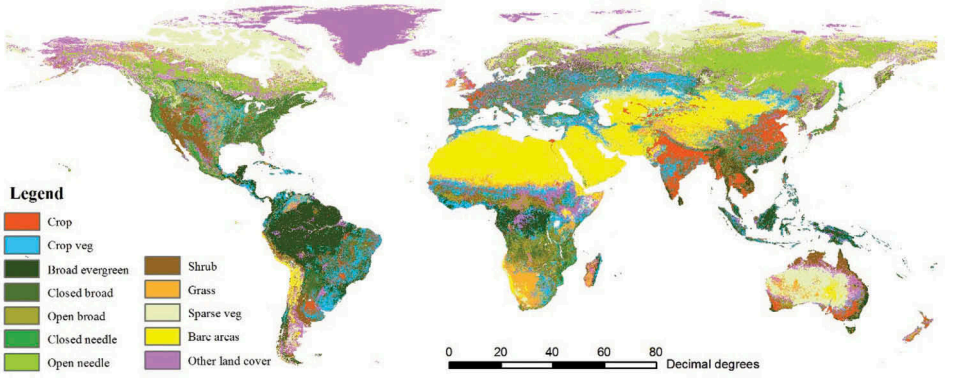


**Figure 2.** Distribution of the typical land-cover types.

these trends accounted for 37.27% and 7.98% of the pixels, respectively. Meanwhile, 54.75% of the pixels showed insignificant changes, 34.85% showed apparent greening, and 19.90% showed browning, thus yielding a ratio of about 1.7:1 (Figure 3). These data suggest that more revegetation occurred within the insignificant trends than significant variation. As more than half of the NDVI changes were insignificant,

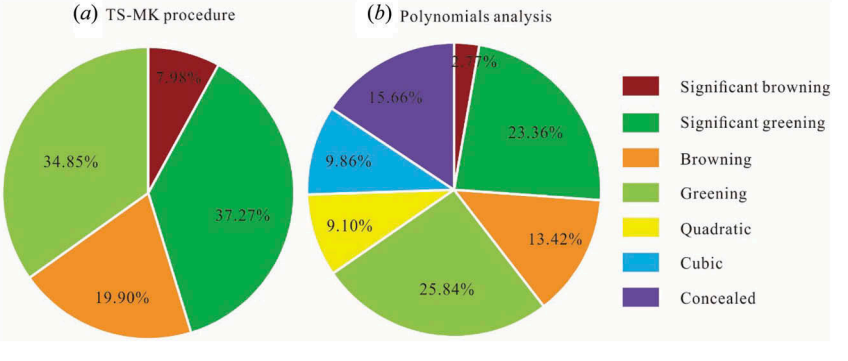


**Figure 3.** Differences in the trend classification results between the traditional TS–MK (Theil–Sen and Mann–Kendall) procedure and the proposed polynomial analysis by stepwise regression.

more detailed change trends should be quantified. After separation of the cubic and quadratic types, significant linear variation pixels were reduced to 26.13%, and 9.86% of the pixels showed cubic trends and 9.10% of the pixels showed quadratic trends. Cubic trends were detected for 8.13% of the pixels of up-down-up trends. In comparison, 7.16% of the quadratic trends pixels showed a down-up type. From these results, it can be inferred that many of the pixels classified as 'significant change' pixels by the TS–MK procedure became high-order types because the proportion of significant greening pixels under our polynomial analysis decreased by more than 10–23.36%. Moreover, the percentage of pixels with a concealed trend was 15.66%, which is a considerable proportion of the total 'insignificant change' pixels. In summary, high-order fitting was necessary to accurately characterize the data, as 34.62% of the pixels were reassigned to new variation types in the polynomial analysis.

### 3.2. *Trends on a continental scale*

In general, many of the regions with a high density of human activity experienced revegetation during the 31 years analysed in this study; in contrast, semi-arid areas with sparse vegetation suffered from vegetation degradation (deterioration) (Figure 4). In Europe, India, the northern Amazon basin, western Africa, and northern parts of North America, significant vegetation greening trends were found. In comparison, significant vegetation browning trends were detected mainly in sparse vegetation areas such as western America, northwestern China, and southern Argentina. Furthermore, high-order-type pixels appeared either in moist regions along middle latitudes or near the tundra at high latitudes. This wide distribution pattern reveals that inter-annual non-linear vegetation variations can be detected over relatively large expanses rather than in aggregated local areas.

The statistics for the continental scale also show that there were some differences in the proportions of high-order-type pixels (Figure 5). Asia showed the highest proportion

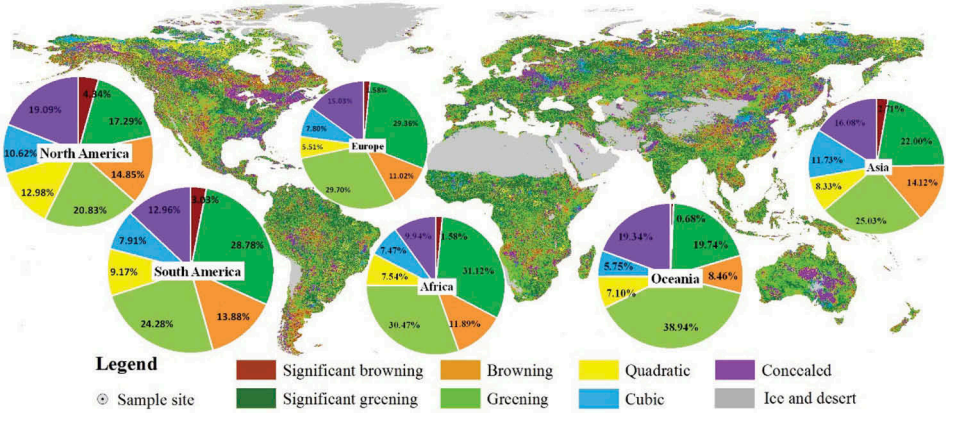


Figure 4. Map of global vegetation dynamics for 1982–2012. Data were obtained through polynomial analyses and statistics on a continental scale; the sample sites were selected artificially to illustrate the forms of different trend types. Asia includes Russia in this figure.

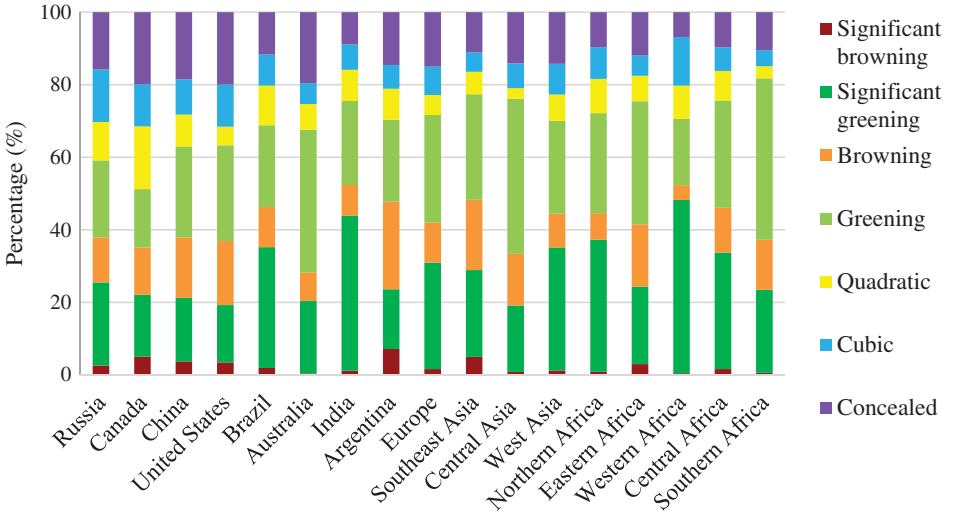


**Figure 5.** Proportions of different vegetation variation types on national and regional scales.

of cubic-trending pixels on a continental scale, with values as high as 11.73%; meanwhile, the percentage was the lowest in Oceania at 5.75%. More than 19% of the pixels in both Oceania and North America showed concealed trends, while the percentage was 9.94% for Africa. Moreover, the proportion of greening pixels was several times larger than the proportion of browning pixels on the continents, and the percentage of significant browning pixels was less than 5%. Therefore, these data suggest that even with extensive human activity, the global NDVI has increased largely because of the increasing trends in cultivated areas.

### 3.3. *Trends on national and regional scales*

Among the eight countries with large areas, the highest percentage of significant greening pixels was found in India at 42.78%, whereas the second highest percentage was 33.28% in Brazil. The percentage of browning pixels in India was 8.43%, which was slightly above the 7.93% observed in Australia; the highest percentage was 24.20% in Argentina. In Canada and USA, there were notable concealed trends that encompassed more than 19% of the pixels, which indicates that cubic or quadratic trends existed whereas the variation had been offset in the overall time frame; in India, only 8.86% of the pixels showed concealed trends. These values could represent differences in the vegetation dynamics observed among the eight analysed countries.

In addition to the eight-country analysis, other territories on the continents were divided into nine regions. In southeastern Asia, the percentage of browning pixels was as high as 19.37%, but it was only 4.05% in western Africa. The similarity of the vegetation variations in western Asia and northern Africa can be explained by the homogeneous land-cover types. Southern Africa had the highest percentage of greening pixels (44.54%); the percentage in central Asia was also high at 42.80%. These data suggest that linear fitting models are particularly ineffective for some regions of Africa, where concealed trends accounted for a small but substantial portion of the data.

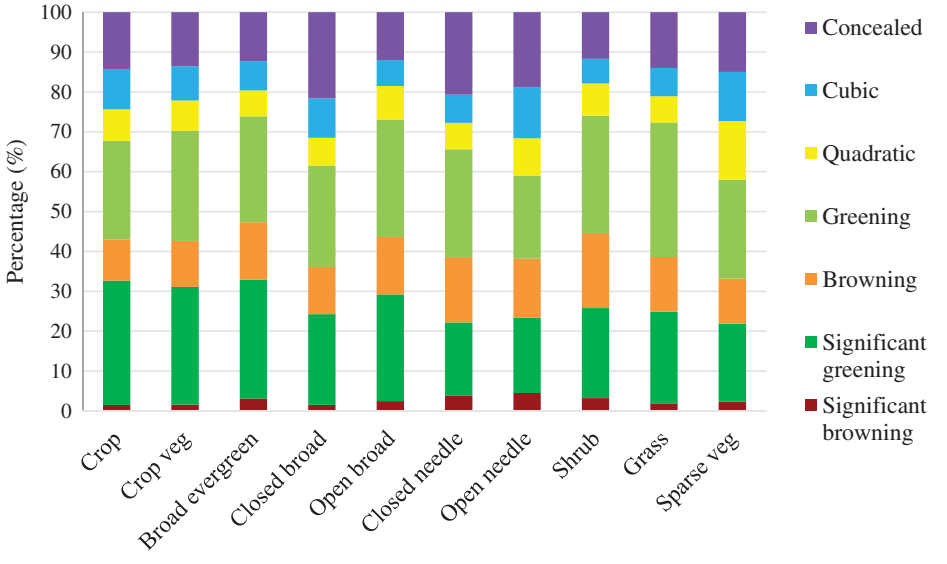


Figure 6. Proportions of vegetation variation types for different land-cover types.

### 3.4. *Differences in trend types with respect to land-cover types*

As vegetation variations are diverse across the different countries and regions, land-cover types should be separated and analysed to determine the contribution of land-cover types to these variations. As expected, the results from our analyses showed apparent differences in the trends among the various land-cover types (Figure 6). The new fitting procedure was most effective for the *sparse veg* and *open needle* land-cover types, as the high-order pixels contributed to more than 40% of the total, and cubic-trending pixels contributed 12.29% and 12.83%, respectively. Moreover, significant greening in the *crop veg* and *crop* land-cover types indicates that cultivated land experienced considerable productivity increases over the 30 year period. More than 20% of the pixels for the *closed needle* and *closed broad* land-cover types showed concealed trends. This means that non-linear trend analysis is certainly needed for this land-cover type to characterize the trends accurately, as latent trends would be lost using the traditional procedure. Moreover, the differences between *broad evergreen* and *closed broad* land-cover types were significant. This phenomenon may be attributed to differences in the local climates, which are the basic driving force of vegetation dynamics. Generally, the vegetation dynamics for most of the land-cover types were effectively quantified with the new procedure. However, some undetermined variations were still present, including a percentage accounting for more than 45% of 'insignificant change' pixels in the *shrub* and *grass* land-cover types.

## 4. Discussion

### 4.1. *Sensitivity of the fitting curves*

To observe the ideal fitting curves for each trend type, random sample sites were selected for further evaluation with the polynomial analysis procedure (Figure 7). At

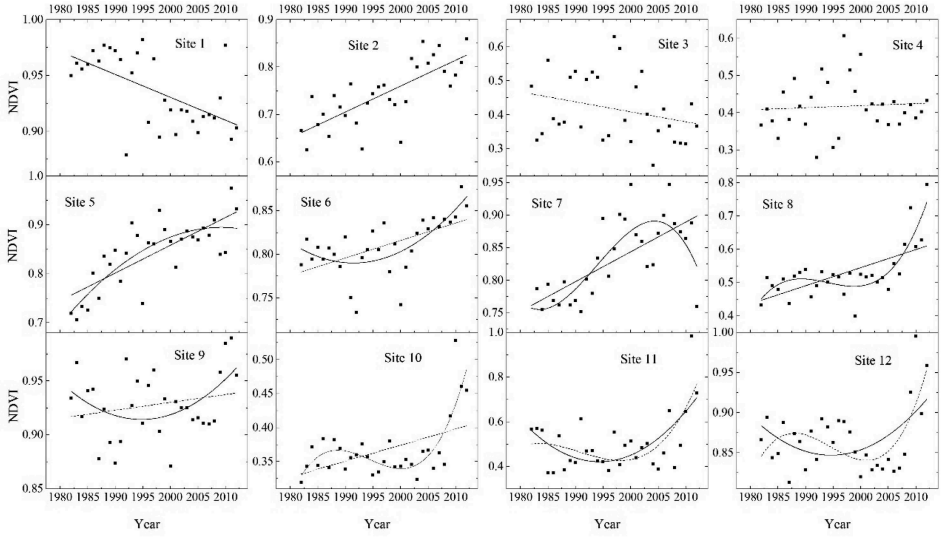


**Figure 7.** Fitting curves for sample sites with different vegetation variation types (NDVI: normalized difference vegetation index). Site 1: – open needle-leaved deciduous or evergreen forest; site 2 –irrigated croplands; site 3 – bare areas; site 4 – closed to open grassland; site 5, site 7, site 8 – rain-fed croplands; site 6 – open broad-leaved deciduous forest; site 9 – closed broad-leaved deciduous forest; site 10, site 11 – sparse vegetation; site 12 – mosaic croplands/vegetation.

sites 1 and 2, significant greening or browning trends were obvious and the fit was linear. At sites 3 and 4, an almost stochastic allocation appeared with an ambiguous distribution. At sites 5 and 6, quadratic trends with both down-up and up-down patterns were better fits than linear trends. Therefore, if the linear fitting method had been adopted, rapid vegetation variations would have been underestimated and trends would have appeared similar to those at sites 1 and 2. Likewise, at sites 7 and 8, cubic trends with up-down-up and down-up-down patterns were observed; these consisted of two points of inflection for each curve. These trends would have been obscured had OLS linear regression been used, but the complex variations were notable with the high-order regression analysis.

The most persuasive samples were at sites 9 and 10, where the concealed trends would not have passed the significance test in the TS–MK linear regression. In fact, the fast browning during the 1980s at site 9 and the fast greening after 2008 at site 10 were remarkable and should not be neglected. Nevertheless, some high-order trends still existed that could not be fitted by the high-order analysis, such as those at sites 15 and 16. In a sensitivity analysis, we found that when a biquadratic trend was added, 1.92%, 3.64%, and 5.74% of pixels classified as showing quadratic, cubic, and 'insignificant change' trends, respectively, were reclassified as showing biquadratic trends. These reassignment quantities are not considered to represent a large amount because when a cubic trend was added to a hypothetical quadratic classification, 19.90% of the pixels were reassigned. We did not attempt to quantify these higher-order curves as too short an interval was used to achieve a quantitative analysis that would have meaningful ecological implications.

### 4.2. *Implications for the driving forces*

The contribution of polynomial analysis to the detection of vegetation dynamics was remarkable as the high-order fitting method not only raised the regression accuracy but also endowed the curves with more ecological relevance in that vegetation degradation (deterioration) and revegetation appeared at different times in the high-order curves. Vegetation degradation mostly occurred in semi-arid regions (Figure 4). As shown by Fensholt et al. (2012), there is a good correspondence between vegetation dynamics and precipitation in most semi-arid areas; the notable exception here is that negative vegetation trends appeared with positive precipitation trends in southern Argentina. Besides rainfall, some national afforestation programmes likely had an important role in the vegetation growth (Piao et al. 2015). However, global vegetation growth cannot be merely the result of afforestation; in particular, several regions dominated by agriculture had increasing NDVI trends, which was likely due to human influences rather than climatic variables.

Other variation trends may be useful for forecasting the collapse of ecosystems, especially where there is no confidence that the vegetation would recover after a sharp period of deterioration. Urbanization with significant land-cover change was a major force of vegetation deterioration, and the vegetation greenness was more likely to decrease in the exurban and suburban areas than in the highly urban and urban core areas (Zhou et al. 2014). Change in these areas was pronounced and often worse than in cropland-occupied areas, i.e. 2.3 million $km^2$ of forest was lost globally during 2000–2012 (Hansen et al. 2013). The losses of subtropical forests were largely consistent with the pattern of browning trends shown in Figure 4. Although bush encroachment and regeneration of secondary forest showed some revegetation trends, the former ecosystem functions likely have been transformed (Fensholt et al. 2015). In other words, although some variation trends indicative of revegetation after deterioration were observed, these were probably the result of regeneration via different vegetation types after a collapse, rather than a reversion to the previous state.

### 4.3. *Limitations*

A key point that should be highlighted is that the polynomial analysis procedure described here is by no means the only such technique that can be applied in vegetation dynamic analyses; in fact, a diverse range of both regression methods and significance tests can be used. The analysis presented in this article was applied to find the most 'acceptable' trends rather than the most 'accurate' trends. While we obtained more accurate fitting results with higher-order functions, additional evidence is required to confirm the Earth observation trends. In this regard, we intend to highlight the advantages of effective trend fitting for our polynomial analysis rather than claim that our procedure outperforms earlier techniques in all respects.

The uncertainties derived from data sources and from trend-fitting methods should be separated. Although some inter-comparisons among different NDVI products have been performed (Scheftic et al. 2014; Tarnavsky, Garrigues, and Brown 2008), the differences in inter-annual NDVI fitting trends among the various NDVI products are

still unclear and would benefit from further attention. To better illustrate the ecological implications of changes in vegetation, the results of our polynomial analysis emphasize the utility of returning to high-order regressions based on the widely used TS–MK procedure. However, as Fensholt et al. (2015) demonstrated that if different data-processing methods are introduced, some inconsistent trends are to be expected.

The polynomial regression procedure described here does have a drawback in that trends cannot be extended far into the future, as fitting results may depend on the period studied in the analysis. Thus, this type of research can only document vegetation growth in past records rather than forecast future vegetation variations. Importantly, however, our method can detect some ecological processes over a 30 year timescale, and vegetation deterioration or revegetation trends were observed successfully. The algorithm applied in this study is reasonable because the study period was larger than one or two vegetation deterioration or revegetation periods. In other words, because we used a relatively long time series, there was a low amount of uncertainty in the model results. In future research, applying ecological models to simulate future vegetation dynamics would be helpful for understanding global change. Our studies on past changes would therefore be informative for the development of such ecological models.

## 5. Conclusion

In this study, a polynomial trend-fitting method that uses stepwise regression was proposed for mapping vegetation dynamics. Vegetation variations were classified into cubic, quadratic, linear, and concealed trends. Based on the GIMMS3g NDVI data set, 31 years of global vegetation dynamics were mapped. We found that 34.62% of the pixels could be assigned to new variation types under the polynomial analysis compared with the traditional TS–MK procedure. Additionally, 15.66% of the pixels with concealed trends were formerly defined as 'insignificant change' pixels. In particular, Asia had the highest proportion of cubic-trending pixels on a continental scale, which amounted to 11.73% of the total, and Canada had the highest proportion of quadratic-trending pixels (17.28%) among all of the large countries studied. Moreover, up to 30% of the cultivated land cover showed significant greening in the NDVI data, thus indicating considerable global agriculture production growth over the study period. The *closed needle* and *closed broad* forest-cover types showed the highest proportion of concealed-trending pixels, which amounted to 20%. Vegetation degradation and revegetation trends were identified successfully using this polynomial analysis, and such changes could have important ecological implications. Overall, this polynomial analysis procedure was valuable for identifying non-linear trends in vegetation dynamics. In future research, inter-comparisons of annual NDVI trends among different NDVI products are needed, and other non-linear trend-fitting methods should be investigated to monitor global land changes more effectively.

## Disclosure statement

No potential conflict of interest was reported by the authors.

## Funding

This work was supported by the National Natural Science Foundation of China [41330747];

## References

Alcaraz-Segura, D., E. Chuvieco, H. E. Epstein, E. S. Kasischke, and A. Trishchenko. 2010. "Debating the Greening vs. Browning of the North American Boreal Forest: Differences between Satellite Datasets." *Global Change Biology* 16 (2): 760–770. doi:10.1111/j.1365-2486.2009.01956.x.

Bao, G., Z. H. Qin, Y. H. Bao, Y. Zhou, W. J. Li, and A. Sanjjav. 2014. "NDVI-Based Long-Term Vegetation Dynamics and Its Response to Climatic Change in the Mongolian Plateau." *Remote Sensing* 6 (9): 8337–8358. doi:10.3390/Rs6098337.

Beck, H. E., T. R. McVicar, A. I. J. M. van Dijk, J. Schellekens, R. A. M. De Jeu, and L. A. Bruijnzeel. 2011. "Global Evaluation of Four AVHRR-NDVI Data Sets: Intercomparison and Assessment against Landsat Imagery." *Remote Sensing of Environment* 115 (10): 2547–2563. doi:10.1016/j.rse.2011.05.012.

Bicheron, P., V. Amberg, L. Bourg, D. Petit, M. Huc, B. Miras, C. Brockmann, O. Hagolle, S. Delwart, F. Ranera, M. Leroy, O. Arino. 2011. "Geolocation Assessment of MERIS GlobCover Orthorectified Products." *IEEE Transactions on Geoscience and Remote Sensing* 49 (8): 2972–2982. doi:10.1109/TGRS.2011.2122337.

Cañón, J., F. Domínguez, and J. B. Valdes. 2011. "Vegetation Responses to Precipitation and Temperature: A Spatiotemporal Analysis of Ecoregions in the Colorado River Basin." *International Journal of Remote Sensing* 32 (20): 5665–5687. doi:10.1080/01431161.2010.507259.

de Jong, R., S. de Bruin, A. de Wit, M. E. Schaepman, and D. L. Dent. 2011. "Analysis of Monotonic Greening and Browning Trends from Global NDVI Time-Series." *Remote Sensing of Environment* 115 (2): 692–702. doi:10.1016/j.rse.2010.10.011.

de Jong, R., J. Verbesselt, A. Zeileis, and M. E. Schaepman. 2013. "Shifts in Global Vegetation Activity Trends." *Remote Sensing* 5 (3): 1117–1133. doi:10.3390/Rs5031117.

Fensholt, R., S. Horion, T. Tagesson, A. Ehammer, E. Ivits, and K. Rasmussen. 2015. "Global-Scale Mapping of Changes in Ecosystem Functioning from Earth Observation-Based Trends in Total and Recurrent Vegetation." *Global Ecology and Biogeography* 24 (9): 1003–1017. doi:10.1111/geb.12338.

Fensholt, R., T. Langanke, K. Rasmussen, A. Reenberg, S. D. Prince, C. Tucker, R. J. Scholes, et al. 2012. "Greenness in Semi-Arid Areas across the Globe 1981-2007 - an Earth Observing Satellite Based Analysis of Trends and Drivers." *Remote Sensing of Environment* 121: 144–158. doi:10.1016/j.rse.2012.01.017.

Fensholt, R., and S. R. Proud. 2012. "Evaluation of Earth Observation Based Global Long Term Vegetation Trends - Comparing GIMMS and MODIS Global NDVI Time Series." *Remote Sensing of Environment* 119: 131–147. doi:10.1016/j.rse.2011.12.015.

Fernandes, R., and S. G. Leblanc. 2005. "Parametric (Modified Least Squares) and Non-Parametric (Theil-Sen) Linear Regressions for Predicting Biophysical Parameters in the Presence of Measurement Errors." *Remote Sensing of Environment* 95 (3): 303–316. doi:10.1016/j.rse.2005.01.005.

Forkel, M., N. Carvalhais, J. Verbesselt, M. D. Mahecha, C. Neigh, and M. Reichstein. 2013. "Trend Change Detection in NDVI Time Series: Effects of Inter-Annual Variability and Methodology." *Remote Sensing* 5 (5): 2113–2144. doi:10.3390/rs5052113.

Fuller, D. O., and Y. Wang. 2014. "Recent Trends in Satellite Vegetation Index Observations Indicate Decreasing Vegetation Biomass in the Southeastern Saline Everglades Wetlands." *Wetlands* 34 (1): 67–77. doi:10.1007/s13157-013-0483-0.

Gao, Y., J. Huang, S. Li, and S. C. Li. 2012. "Spatial Pattern of Non-Stationarity and Scale-Dependent Relationships between NDVI and Climatic Factors-A Case Study in Qinghai-Tibet Plateau, China." *Ecological Indicators* 20: 170–176. doi:10.1016/j.ecolind.2012.02.007.

Guay, K. C., P. S. A. Beck, L. T. Berner, S. J. Goetz, A. Baccini, and W. Buermann. 2014. "Vegetation Productivity Patterns at High Northern Latitudes: A Multi-Sensor Satellite Data Assessment." *Global Change Biology* 20 (10): 3147–3158. doi:10.1111/Gcb.12647.

Hansen, M. C., P. V. Potapov, R. Moore, M. Hancher, S. A. Turubanova, A. Tyukavina, D. Thau, et al. 2013. "High-Resolution Global Maps of 21st-Century Forest Cover Change." *Science* 342 (6160): 850–853. doi:10.1126/science.1244693.

Holben, B. N. 1986. "Characteristics of Maximum-Value Composite Images from Temporal AVHRR Data." *International Journal of Remote Sensing* 7 (11): 1417–1434. doi:10.1080/01431168608948945.

Hwang, T., C. H. Song, P. V. Bolstad, and L. E. Band. 2011. "Downscaling Real-Time Vegetation Dynamics by Fusing Multi-Temporal MODIS and Landsat NDVI in Topographically Complex Terrain." *Remote Sensing of Environment* 115 (10): 2499–2512. doi:10.1016/j.rse.2011.05.010.

Jamali, S., J. Seaquist, L. Eklundh, and J. Ardö. 2014. "Automated Mapping of Vegetation Trends with Polynomials Using NDVI Imagery over the Sahel." *Remote Sensing of Environment* 141: 79–89. doi:10.1016/j.rse.2013.10.019.

Jiang, N., W. Q. Zhu, Z. T. Zheng, G. S. Chen, and D. Q. Fan. 2013. "A Comparative Analysis between GIMSS Ndvig and Ndvi3g for Monitoring Vegetation Activity Change in the Northern Hemisphere during 1982-2008." *Remote Sensing* 5 (8): 4031–4044. doi:10.3390/Rs5084031.

Ju, J. C., D. P. Roy, Y. M. Shuai, and C. Schaaf. 2010. "Development of an Approach for Generation of Temporally Complete Daily Nadir MODIS Reflectance Time Series." *Remote Sensing of Environment* 114 (1): 1–20. doi:10.1016/j.rse.2009.05.022.

Kandasamy, S., F. Baret, A. Verger, P. Neveux, and M. Weiss. 2013. "A Comparison of Methods for Smoothing and Gap Filling Time Series of Remote Sensing Observations – Application to MODIS LAI Products." *Biogeosciences* 10 (6): 4055–4071. doi:10.5194/bg-10-4055-2013.

Kendall, M. G. 1962. *Rank Correlation Methods*. New York: Hafner.

Kendall, M. G. 1975. *Rank Correlation Methods*. London: Charles Griffin.

Kleynhans, W., J. C. Olivier, K. J. Wessels, F. van den Bergh, B. P. Salmon, and K. C. Steenkamp. 2010. "Improving Land Cover Class Separation Using an Extended Kalman Filter on MODIS NDVI Time-Series Data." *IEEE Geoscience and Remote Sensing Letters* 7 (2): 381–385. doi:10.1109/LGRS.2009.2036578.

Lanorte, A., R. Lasaponara, M. Lovallo, and L. Telesca. 2014. "Fisher-Shannon Information Plane Analysis of SPOT/VEGETATION Normalized Difference Vegetation Index (NDVI) Time Series to Characterize Vegetation Recovery after Fire Disturbance." *International Journal of Applied Earth Observation and Geoinformation* 26: 441–446. doi:10.1016/j.jag.2013.05.008.

Li, S. S., J. P. Yan, X. Y. Liu, and J. Wan. 2013. "Response of Vegetation Restoration to Climate Change and Human Activities in Shaanxi-Gansu-Ningxia Region." *Journal of Geographical Sciences* 23 (1): 98–112. doi:10.1007/s11442-013-0996-8.

Liu, X. F., X. F. Zhu, W. Q. Zhu, Y. Z. Pan, C. Zhang, and D. H. Zhang. 2014. "Changes in Spring Phenology in the Three-Rivers Headwater Region from 1999 to 2013." *Remote Sensing* 6 (9): 9130–9144. doi:10.3390/Rs6099130.

Ma, X. L., A. Huete, Q. Yu, N. R. Coupe, K. Davies, M. Broich, P. Ratana, et al. 2013. "Spatial Patterns and Temporal Dynamics in Savanna Vegetation Phenology across the North Australian Tropical Transect." *Remote Sensing of Environment* 139: 97–115. doi:10.1016/j.rse.2013.07.030.

Mann, H. B. 1945. "Nonparametric Tests against Trend." *Econometrica* 13 (3): 245–259. doi:10.2307/1907187.

Mao, D. H., Z. M. Wang, L. Luo, and C. Y. Ren. 2012. "Integrating AVHRR and MODIS Data to Monitor NDVI Changes and Their Relationships with Climatic Parameters in Northeast China." *International Journal of Applied Earth Observation And Geoinformation* 18: 528–536. doi:10.1016/j.jag.2011.10.007.

Martínez, B., and M. A. Gilabert. 2009. "Vegetation Dynamics from NDVI Time Series Analysis Using the Wavelet Transform." *Remote Sensing of Environment* 113 (9): 1823–1842. doi:10.1016/j.rse.2009.04.016.

Mishra, N. B., K. A. Crews, and A. L. Neuenschwander. 2012. "Sensitivity of EVI-Based Harmonic Regression to Temporal Resolution in the Lower Okavango Delta." *International Journal of Remote Sensing* 33 (24): 7703–7726. doi:10.1080/01431161.2012.701348.

Neeti, N., and J. R. Eastman. 2011. "A Contextual Mann-Kendall Approach for the Assessment of Trend Significance in Image Time Series." *Transactions In Gis* 15 (5): 599–611. doi:10.1111/j.1467-9671.2011.01280.x.

Nemani, R. R., C. D. Keeling, H. Hashimoto, W. M. Jolly, S. C. Piper, C. J. Tucker, R. B. Myneni, and S. W. Running. 2003. "Climate-Driven Increases in Global Terrestrial Net Primary Production from 1982 to 1999." *Science* 300 (5625): 1560–1563. doi:10.1126/science.1082750.

Nie, Q., J. H. Xu, M. H. Ji, L. Cao, Y. Yang, and Y. L. Hong. 2012. "The Vegetation Coverage Dynamic Coupling with Climatic Factors in Northeast China Transect." *Environmental Management* 50 (3): 405–417. doi:10.1007/s00267-012-9885-7.

Peng, J., Z. H. Liu, Y. H. Liu, J. S. Wu, and Y. A. Han. 2012. "Trend Analysis of Vegetation Dynamics in Qinghai-Tibet Plateau Using Hurst Exponent." *Ecological Indicators* 14 (1): 28–39. doi:10.1016/j.ecolind.2011.08.011.

Piao, S. L., G. D. Yin, J. G. Tan, L. Cheng, M. T. Huang, Y. Li, R. G. Liu, et al. 2015. "Detection and Attribution of Vegetation Greening Trend in China over the Last 30 Years." *Global Change Biology* 21 (4): 1601–1609. doi:10.1111/gcb.12795.

Rios, R. A., L. Parrott, H. Lange, and R. F. De Mello. 2015. "Estimating Determinism Rates to Detect Patterns in Geospatial Datasets." *Remote Sensing of Environment* 156: 11–20. doi:10.1016/j.rse.2014.09.019.

Rocchini, D., and A. Vannini. 2010. "What is Up? Testing Spectral Heterogeneity versus NDVI Relationship Using Quantile Regression." *International Journal of Remote Sensing* 31 (10): 2745–2756. doi:10.1080/01431160903085651.

Running, S. W., R. R. Nemani, F. A. Heinsch, M. S. Zhao, M. Reeves, and H. Hashimoto. 2004. "A Continuous Satellite-Derived Measure of Global Terrestrial Primary Production." *Bioscience* 54 (6): 547–560. doi:10.1641/0006-3568(2004)054[0547:Acsmog]2.0.Co;2.

Scheftic, W., X. B. Zeng, P. Broxton, and M. Brunke. 2014. "Intercomparison of seven NDVI Products over the United States and Mexico." *Remote Sensing* 6 (2): 1057–1084. doi:10.3390/Rs6021057.

Schucknecht, A., S. Erasmi, I. Niemeyer, and J. Matschullat. 2013. "Assessing Vegetation Variability and Trends in North-Eastern Brazil Using AVHRR and MODIS NDVI Time Series." *European Journal of Remote Sensing* 46: 40–59. doi:10.5721/Eujrs20134603.

Sen, P. K. 1968. "Estimates of the Regression Coefficient Based on Kendall's Tau." *Journal of the American Statistical Association* 63 (324): 1379–1389. doi:10.1080/01621459.1968.10480934.

Steven, M. D., T. J. Malthus, F. Baret, H. Xu, and M. J. Chopping. 2003. "Intercalibration of Vegetation Indices from Different Sensor Systems." *Remote Sensing of Environment* 88 (4): 412–422. doi:10.1016/j.rse.2003.08.010.

Stow, D., A. Petersen, A. Hope, R. Engstrom, and L. Coulter. 2007. "Greenness Trends of Arctic Tundra Vegetation in the 1990s: Comparison of Two NDVI Data Sets from NOAA AVHRR Systems." *International Journal of Remote Sensing* 28 (21): 4807–4822. doi:10.1080/01431160701264284.

Tarnavsky, E., S. Garrigues, and M. E. Brown. 2008. "Multiscale Geostatistical Analysis of AVHRR, SPOT-VGT, and MODIS Global NDVI Products." *Remote Sensing of Environment* 112 (2): 535–549. doi:10.1016/j.rse.2007.05.008.

Theil, H. 1950. "A Rank-Invariant Method of Linear and Polynomial Regression Analysis, I, II and III." *Proceedings of the Royal Netherlands Academy of Sciences* 53: 386–392, 521–525, 1397–1412.

Tian, F., R. Fensholt, J. Verbesselt, K. Grogan, S. Horion, and Y. J. Wang. 2015. "Evaluating Temporal Consistency of Long-Term Global NDVI Datasets for Trend Analysis." *Remote Sensing of Environment* 163: 326–340. doi:10.1016/j.rse.2015.03.031.

Tucker, C. J. 1979. "Red and Photographic Infrared Linear Combinations for Monitoring Vegetation." *Remote Sensing of Environment* 8 (2): 127–150. doi:10.1016/0034-4257(79)90013-0.

Tucker, C. J., J. E. Pinzon, M. E. Brown, D. A. Slayback, E. W. Pak, R. Mahoney, E. F. Vermote, and N. El Saleous. 2005. "An Extended AVHRR 8-Km NDVI Dataset Compatible with MODIS and SPOT

Vegetation NDVI Data." *International Journal of Remote Sensing* 26 (20): 4485–4498. doi:10.1080/01431160500168686.

Tucker, C. J., D. A. Slayback, J. E. Pinzon, S. O. Los, R. B. Myneni, and M. G. Taylor. 2001. "Higher Northern Latitude Normalized Difference Vegetation Index and Growing Season Trends from 1982 to 1999." *International Journal of Biometeorology* 45 (4): 184–190. doi:10.1007/s00484-001-0109-8.

Verbesselt, J., R. Hyndman, G. Newnham, and D. Culvenor. 2010a. "Detecting Trend and Seasonal Changes in Satellite Image Time Series." *Remote Sensing of Environment* 114 (1): 106–115. doi:10.1016/j.rse.2009.08.014.

Verbesselt, J., R. Hyndman, A. Zeileis, and D. Culvenor. 2010b. "Phenological Change Detection while Accounting for Abrupt and Gradual Trends in Satellite Image Time Series." *Remote Sensing of Environment* 114 (12): 2970–2980. doi:10.1016/j.rse.2010.08.003.

Verbesselt, J., A. Zeileis, and M. Herold. 2012. "Near Real-Time Disturbance Detection Using Satellite Image Time Series." *Remote Sensing of Environment* 123: 98–108. doi:10.1016/j.rse.2012.02.022.

Weiss, J. L., D. S. Gutzler, J. E. A. Coonrod, and C. N. Dahm. 2004. "Long-Term Vegetation Monitoring with NDVI in a Diverse Semi-Arid Setting, Central New Mexico, USA." *Journal of Arid Environments* 58 (2): 249–272. doi:10.1016/j.jaridenv.2003.07.001.

Wessels, K. J., F. van den Bergh, and R. J. Scholes. 2012. "Limits to Detectability of Land Degradation by Trend Analysis of Vegetation Index Data." *Remote Sensing of Environment* 125: 10–22. doi:10.1016/j.rse.2012.06.022.

Yan, E. P., G. X. Wang, H. Lin, C. Z. Xia, and H. Sun. 2015. "Phenology-Based Classification of Vegetation Cover Types in Northeast China Using MODIS NDVI and EVI Time Series." *International Journal of Remote Sensing* 36 (2): 489–512. doi:10.1080/01431161.2014.999167.

Zhou, D. C., S. Q. Zhao, S. G. Liu, and L. X. Zhang. 2014. "Spatiotemporal Trends of Terrestrial Vegetation Activity along the Urban Development Intensity Gradient in China's 32 Major Cities." *Science of the Total Environment* 488–489: 136–145. doi:10.1016/j.scitotenv2014.04.080.